MECH. STRUCT. & MACH., 27(3), 275–292 (1999)

Automated Optimal Stiffener Pattern Design*

Hae Chang Gea and Jianhui Luo

DEPARTMENT OF MECHANICAL AND AEROSPACE ENGINEERING
RUTGERS, THE STATE UNIVERSITY OF NEW JERSEY
PISCATAWAY, NJ 08855-0909, U.S.A

ABSTRACT

An automated topology optimization based approach is proposed to generate the optimal stiffener pattern of 3D shell structures with the objective of maximizing a band of eigenfrequencies. The methodology is based on a fiber-reinforced composite model in which the stiffeners and base structure are modeled as fibers and matrix, respectively. Solutions to the optimization problem are obtained by means of an iterative, two-level procedure based on an optimality criterion approach and a method of mathematical programming using analytical sensitivity analysis. Two numerical examples are presented to demonstrate the effectiveness of the proposed approach.

I. INTRODUCTION

During the past few decades, one of the most important research topics in structural design is how to design the stiffest structure, under weight constraints. A typical example of this is the design of stiffened shell structures. Shell structures exhibit poor stiffness and NVH (Noise, Vibration, and Harshness) performance. Due to their flexibility, they require stiffeners to supplement their rigidities. To achieve the highest stiffness, stiffeners must be placed and oriented in

*Communicated by S. Azarm

an optimal way. Although the design of stiffeners is of long interest to engineers, there is still no systematic tool available. Their design has been accomplished so far through an experience-based, trial-and-error process. With the development of structural optimization, it is now possible to automate the design process of stiffened shell structures that can increase the productivity and efficiency of designers.

There are two research topics related to the stiffener pattern design; the reinforcement problem and the composite structure optimization problem. The topology optimization approach has been successfully applied to deal with the reinforcement problem, in which a given structure is reinforced using a prescribed amount of material (Diaz and Kikuchi 1992; Ma, Kikuchi and Hagiwara 1993). Their work is to find the best location of the stiffening material, using a homogenization method (Bendsøe and Kikuchi 1988), in order to achieve design goals such as natural frequency optimization or frequency response optimization. In the context of the composite structure optimization problem, Pedensen (1989, 1990) proposed a strain based method to calculate the optimal orientation of orthotropic materials, and Thomsen (1991) considered the optimization of 2D composite discs using a simple rule of mixtures.

In this paper, an automated design approach to the optimal stiffener pattern is proposed, for the multiple eigenfrequency optimization of 3D shell structure. The methodology is based on a fiber-reinforced composite model in which the stiffeners and base structure are modeled as fibers and matrix respectively. The Composite Cylinder Assemblage (CCA) model (Hashin and Rosen 1964) is applied to evaluate elastic constants of the composite. By inserting a prescribed amount of fiber into the base structure, the optimal stiffener pattern can be determined by the final distribution of the fibers and their orientations. Solutions to the optimization problem are obtained by means of an iterative, two-level procedure based on an optimality criterion approach and a method of mathematical programming using analytical sensitivity analysis.

The remainder of the paper is organized as follows. Section 2 introduces the CCA model and the analytical representation of effective properties of the fiber-reinforced composite. The problem of maximizing multiple structural eigenvalues is formulated in Section 3. Sensitivity analysis of the objective function with respect to design variables is considered in Section 4. The optimization techniques for solving the problem is discussed in Section 5. Two numerical examples are considered in Section 6, and conclusions are made in Section 7.

II. FIBER-REINFORCED COMPOSITE MODELING OF THE STRUCTURE

The stiffener layout optimization problem can be considered as the optimal placement of a given stiffener material on the base shell material. In order to

account for both stiffener location and orientation, a fiber-reinforced composite model is utilized to simulate the stiffened shell structure. In this model, the design domain is discretized into elements that are made of a composite material consisting of co-aligned fibers embedded in a solid matrix. The fiber phase is treated as the stiffener and the matrix phase as the base shell material. The volume concentration of fibers in each element and their orientation are considered as the design variables. The optimal stiffener pattern can be identified by the final distribution of the fibers and their orientations.

The effective material properties of the fiber-reinforced composite can be derived using the Composite Cylinder Assemblage (CCA) model proposed by Hashin and Rosen (1964). The model is shown in Fig. 1. A composite cylinder is composed of an infinitely long circular fiber of radius a and an annulus of matrix material of radius of b. The absolute values of radii a and b vary with each composite cylinder, such that a volume filling configuration is obtained. The ratio of radii a/b is required to be constant for all composite cylinders. The fiber direction is axis 1. The axial Young's modulus, the corresponding transverse Poisson's ratio, the plane strain bulk modulus, and the axial shear modulus are given as

$$E_{11} = cE_f + (1 - c)E_m + \frac{4c(1 - c)(\nu_f - \nu_m)^2\mu_m}{[(1 - c)\mu_m/(k_f + \mu_f/3)] + [c\mu_m/(k_m + \mu_m/3)] + 1} \tag{1}$$

$$\nu_{12} = (1 - c)\nu_m + c\nu_f + \frac{c(1 - c)(\nu_f - \nu_m)[\mu_m/(k_m + \mu_m/3) - \mu_m/(k_f + \mu_f/3)]}{[(1 - c)\mu_m/(k_f + \mu_f/3)] + [c\mu_m/(k_m + \mu_m/3)] + 1} \tag{2}$$

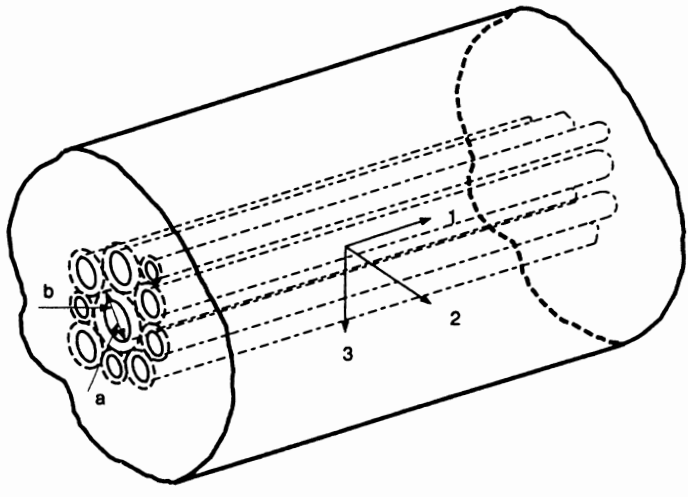

Fig. 1. Composite cylinder assembly model.

$$K_{23} = k_m + \frac{\mu_m}{3} + \frac{c}{1/[k_f - k_m + \frac{1}{3}(\mu_f - \mu_m)] + (1-c)/\left(k_m + \frac{4}{3}\mu_m\right)} \tag{3}$$

$$\mu_{12} = \frac{\mu_f(1+c) + \mu_m(1-c)}{\mu_f(1-c) + \mu_m(1+c)}\mu_m \tag{4}$$

where c is the volume fraction of the fiber phase, k and μ denote bulk modulus and shear modulus, respectively, and indices f and m represent fiber phase and matrix phase. The fifth property, the transverse shear modulus μ_{23}, can be obtained by solving the following equation (Christensen and Lo, 1979):

$$A\left(\frac{\mu_{23}}{\mu_m}\right)^2 + 2B\left(\frac{\mu_{23}}{\mu_m}\right) + C = 0 \tag{5}$$

where A, B, and C are parameters determined by the material properties of the fiber and matrix phase. Detailed expressions are given by Christensen and Lo (1979). The transverse Young's modulus can be obtained from the following relation:

$$\frac{1}{E_{22}} = \frac{\nu_{12}^2}{E_{11}} + \frac{1}{4}\left(\frac{1}{\mu_{23}} + \frac{1}{K_{23}}\right) \tag{6}$$

The density of fiber-reinforced material ρ can be represented in terms of fiber density ρ_f, matrix density ρ_m, and fiber volume concentration c as

$$\rho = c\rho_f + (1-c)\rho_m \tag{7}$$

Once the effective material properties of the fiber-reinforced composite have been determined, they can be utilized to calculate the stiffness matrix, yielding

$$\begin{Bmatrix} \sigma_1 \\ \sigma_2 \\ \sigma_{12} \\ \sigma_{23} \\ \sigma_{13} \end{Bmatrix} = \begin{bmatrix} \frac{E_{11}^2}{E_{11} - E_{22}\nu_{12}^2} & \frac{\nu_{12}E_{11}E_{22}}{E_{11} - E_{22}\nu_{12}^2} & 0 & 0 & 0 \\ \frac{\nu_{12}E_{11}E_{22}}{E_{11} - E_{22}\nu_{12}^2} & \frac{E_{11}E_{22}}{E_{11} - E_{22}\nu_{12}^2} & 0 & 0 & 0 \\ 0 & 0 & \mu_{12} & 0 & 0 \\ 0 & 0 & 0 & \mu_{23} & 0 \\ 0 & 0 & 0 & 0 & \mu_{12} \end{bmatrix} \begin{Bmatrix} \varepsilon_1 \\ \varepsilon_2 \\ \gamma_{12} \\ \gamma_{23} \\ \gamma_{13} \end{Bmatrix} \tag{8}$$

The stiffness matrix in Eq. 8 corresponds to the case in which the fiber orientation collides with the global coordinate system, and is denoted as $\boldsymbol{C}_0$. If the fiber rotates through an angle θ with respect to the global coordinate system, the resulting stiffness matrix $\boldsymbol{C}$ can be obtained through the following standard relationship:

$$\boldsymbol{C} = \boldsymbol{T}^T(\theta)\boldsymbol{C}_0\boldsymbol{T}(\theta) \tag{9}$$

where $\boldsymbol{T}(\theta)$ is in the form of

$$\boldsymbol{T}(\theta) = \begin{bmatrix} \cos^2\theta & \sin^2\theta & \cos\theta\sin\theta & 0 & 0 \\ \sin^2\theta & \cos^2\theta & -\cos\theta\sin\theta & 0 & 0 \\ -2\cos\theta\sin\theta & 2\cos\theta\sin\theta & \cos^2\theta - \sin^2\theta & 0 & 0 \\ 0 & 0 & 0 & \cos\theta & \sin\theta \\ 0 & 0 & 0 & -\sin\theta & \cos\theta \end{bmatrix} \tag{10}$$

III. MULTIPLE EIGENVALUE OPTIMIZATION

In designing mechanical components with best vibration performance, a band of specified eigenvalues are often required to be elevated to their maximum values. In order to deal with this multiple eigenvalue optimization problem, a mean-eigenvalue Λ, which is a combination of multiple eigenvalues, is defined as the objective function; i.e.,

$$\textit{maximize} \qquad \Lambda = \sum_{i=1}^{m} \lambda_{n_i}/\lambda_{0_i} \tag{11}$$

where λ_{n_i} $(i = 1,2, \cdots, m)$ are the specified eigenvalues, n_i $(i = 1,2, \cdots, m)$ are order numbers of the specified eigenvalues. λ_{0_i} $(i = 1,2, \cdots, m)$ are given parameters that are usually taken as the eigenvalues of the initial design. Inclusion of these weighting coefficients in the expression for Λ is to assure each specified eigenvalues makes a nearly equal contribution to the objective function. Each eigenvalue λ_{n_i} satisfies the following eigenvalue problem:

$$\int_\Omega C_{ijkl} \frac{\partial \phi_i^{n_i}}{\partial x_j} \frac{\partial \psi_k}{\partial x_l} d\Omega - \lambda_{n_i} \int_\Omega \rho \phi_k^{n_i} \psi_k d\Omega = 0 \tag{12}$$

where C_{ijkl} are the elastic coefficients of the composite material, ϕ^{n_i} is the eigenvector corresponding to λ_{n_i}, ρ denotes the material density, and ψ is a virtual system eigenvector in the kinematic-ally admissible set.

Generally, the total weight of add-on material cannot exceed a prescribed amount. This constraint can be stated as

$$W = \int_{\Omega} c\rho_f d\Omega \leq W_0 \tag{13}$$

where ρ_f stands for the density of fiber and W_0 represents the given maximal total mass of the fibers.

A side constraint is also considered for the problem. The fiber concentration in the composite must satisfy

$$0 \leq c \leq 1 \tag{14}$$

In summary, the optimization problem can be stated as follows:

$$\begin{aligned} &\textit{maximize} \quad \Lambda \\ &\textit{subject to:} \quad W \leq W_0 \end{aligned} \tag{15}$$

IV. SENSITIVITY ANALYSIS

The sensitivity of the mean-eigenvalue with respect to a design variable can be obtained as

$$\frac{\partial \Lambda}{\partial b} = \sum_{i=1}^{m} \frac{1}{\lambda_{0_i}} \frac{\partial \lambda_{n_i}}{\partial b} \tag{16}$$

where b can be either of the design variables c and θ, and $\partial\lambda_{n_i}/\partial b$ is the sensitivity of the n_i^{th} eigenvalue with respect to the design variable b, which has the form (Haug, Komkov and Choi 1986)

$$\frac{\partial \lambda_{n_i}}{\partial b} = \int_{\Omega} \frac{\partial C_{ijkl}}{\partial b} \frac{\partial \phi_i^{n_i}}{\partial x_j} \frac{\partial \phi_k^{n_i}}{\partial x_l} d\Omega - \lambda_{n_i} \int_{\Omega} \frac{\partial \rho}{\partial b} (\phi_k^{n_i})^2 d\Omega \tag{17}$$

The above expression is used to calculate the mean-eigenvalue sensitivity with respect to the density design variable c. For the orientation design variable θ, Eq. 17 can be simplified as

$$\frac{\partial \lambda_{n_i}}{\partial \theta} = \int_{\Omega} \frac{\partial C_{ijkl}}{\partial \theta} \frac{\partial \phi_i^{n_i}}{\partial x_j} \frac{\partial \phi_k^{n_i}}{\partial x_l} d\Omega \tag{18}$$

Let $\varepsilon_{ij}^{n_i}$ represents the equivalent strain vector corresponding to the n_i^{th} eigenvector; i.e.,

$$\varepsilon_{ij}^{n_i} = \frac{1}{2}\left(\frac{\partial \phi_i^{n_i}}{\partial x_j} + \frac{\partial \phi_j^{n_i}}{\partial x_i} \right) \tag{19}$$

Equation 18 can then be rewritten as

$$\frac{\partial \lambda_{n_i}}{\partial \theta} = \int_{\Omega} \frac{\partial C_{ijkl}}{\partial \theta} \varepsilon_{ij}^{n_i} \varepsilon_{kl}^{n_i} d\Omega = \int_{\Omega} \boldsymbol{\varepsilon}^{n_i T} \frac{\partial \boldsymbol{C}}{\partial \theta} \boldsymbol{\varepsilon}^{n_i} d\Omega \tag{20}$$

The rotated stiffness matrix $\boldsymbol{C}$ can be decomposed as a planar stiffness matrix $\boldsymbol{C}^0$ and a transverse stiffness matrix $\boldsymbol{C}^1$. The matrices $\boldsymbol{C}^0$ and $\boldsymbol{C}^1$ can be determined from the following relations:

$$\begin{aligned} \boldsymbol{C}^0 &= \boldsymbol{T}_0^{\mathrm{T}}(\theta) \boldsymbol{C}_0^0 \boldsymbol{T}^0(\theta) \\ \boldsymbol{C}^1 &= \boldsymbol{T}_1^{\mathrm{T}}(\theta) \boldsymbol{C}_0^1 \boldsymbol{T}_1(\theta) \end{aligned} \tag{21}$$

where $\boldsymbol{C}_0^0$ and $\boldsymbol{C}_0^1$ are unrotated planar and transverse stiffness matrices, and $\boldsymbol{T}_0$ and $\boldsymbol{T}_1$ are sub-matrices of the standard rotational matrix $\boldsymbol{T}$. They are of the forms

$$\boldsymbol{C}_0^0 = \begin{bmatrix} \dfrac{E_{11}^2}{E_{11} - E_{22}\nu_{12}^2} & \dfrac{\nu_{12} E_{11} E_{22}}{E_{11} - E_{22}\nu_{12}^2} & 0 \\ \dfrac{\nu_{12} E_{11} E_{22}}{E_{11} - E_{22}\nu_{12}^2} & \dfrac{E_{11} E_{22}}{E_{11} - E_{22}\nu_{12}^2} & 0 \\ 0 & 0 & \mu_{12} \end{bmatrix} \qquad \boldsymbol{C}_0^1 = \begin{bmatrix} \mu_{23} & 0 \\ 0 & \mu_{12} \end{bmatrix} \tag{22}$$

$$\boldsymbol{T}_0(\theta) = \begin{bmatrix} \cos^2\theta & \sin^2\theta & \cos\theta\sin\theta \\ \sin^2\theta & \cos^2\theta & -\cos\theta\sin\theta \\ -2\cos\theta\sin\theta & 2\cos\theta\sin\theta & \cos^2\theta - \sin^2\theta \end{bmatrix}$$

$$\boldsymbol{T}_1(\theta) = \begin{bmatrix} \cos\theta & \sin\theta \\ -\sin\theta & \cos\theta \end{bmatrix} \tag{23}$$

In the stiffened shell structure, membrane, bending, and shear effects are considered. If $\boldsymbol{\varepsilon}^{n_i,m}$, $\boldsymbol{\varepsilon}^{n_i,u}$, and $\boldsymbol{\varepsilon}^{n_i,s}$ denote middle-face planar strain, upper-face planar strain, and transverse shear strain corresponding to the n_i^{th} eigenvector of the stiffened shell structure, Eq. 20 can be expressed as

$$\frac{\partial \lambda_{n_i}}{\partial \theta} = \int_A \left(\frac{4}{3} \boldsymbol{\varepsilon}^{n_i,mT} \frac{\partial \boldsymbol{C}^0}{\partial \theta} \boldsymbol{\varepsilon}^{n_i,m} - \frac{2}{3} \boldsymbol{\varepsilon}^{n_i,mT} \frac{\partial \boldsymbol{C}^0}{\partial \theta} \boldsymbol{\varepsilon}^{n_i,u} + \frac{1}{3} \boldsymbol{\varepsilon}^{n_i,uT} \frac{\partial \boldsymbol{C}^0}{\partial \theta} \boldsymbol{\varepsilon}^{n_i,u} + \boldsymbol{\varepsilon}^{n_i,sT} \frac{\partial \boldsymbol{C}^1}{\partial \theta} \boldsymbol{\varepsilon}^{n_i,s} \right) t dA \tag{24}$$

The above integral is over the whole face of shell structure, and t is the shell thickness. If the finite element mesh is fine enough, the strain vectors can be approximated as values at the centroid of each element, and they can be taken out of the integral in Eq. 24. This leads to a rather simple discrete form of Eq. 24, in terms of orientation design variables $\theta_e (e = 1,2, \cdots, nd)$,

$$\frac{\partial \lambda_{n_i}}{\partial \theta_e} = \frac{4}{3} \boldsymbol{\varepsilon}_e^{n_i,mT} \frac{\partial \boldsymbol{C}_e^0}{\partial \theta_e} \boldsymbol{\varepsilon}_e^{n_i,m} V_e - \frac{2}{3} \boldsymbol{\varepsilon}_e^{n_i,mT} \frac{\partial \boldsymbol{C}_e^0}{\partial \theta_e} \boldsymbol{\varepsilon}_e^{n_i,u} V_e + \frac{1}{3} \boldsymbol{\varepsilon}_e^{n_i,uT} \frac{\partial \boldsymbol{C}_e^0}{\partial \theta_e} \boldsymbol{\varepsilon}_e^{n_i,u} V_e + \boldsymbol{\varepsilon}_e^{n_i,sT} \frac{\partial \boldsymbol{C}_e^1}{\partial \theta_e} \boldsymbol{\varepsilon}_e^{n_i,s} V_e \tag{25}$$

where $\boldsymbol{\varepsilon}_e^{n_i,m}$, $\boldsymbol{\varepsilon}_e^{n_i,u}$, and $\boldsymbol{\varepsilon}_e^{n_i,s}$ are strain vectors at the centroid of the e^{th} design element, $\boldsymbol{C}_e^0$ and $\boldsymbol{C}_e^1$ are rotated planar and transverse stiffness matrices of the e^{th} design cell, and V_e is the element volume. In general, strain vectors $\boldsymbol{\varepsilon}_e^{n_i,m}$, $\boldsymbol{\varepsilon}_e^{n_i,u}$, and $\boldsymbol{\varepsilon}_e^{n_i,s}$ are implicit functions of all the orientation variables, throughout the design space. They thus experience fluctuations with variations of $\theta_e (e = 1,2, \cdots, nd)$.

In this paper, instead of applying the strain based method (Pedensen 1989, 1990), which assumes the strain field is invariable with respect to the orientation variables or the stress based method (Diaz and Bendsøe 1992, Cheng, Kikuchi and Ma 1994) which is based on a fixed stress field, the energy based method (Luo and Gea 1998) is used to explore the dependencies of strain filed on the orientation variables. They are

$$\begin{aligned}
\boldsymbol{\varepsilon}_e^{n_i,m} &= [\boldsymbol{I} + \alpha \boldsymbol{C}_e^{0-1} (\boldsymbol{C}_{e,0}^0 - \boldsymbol{C}_e^0)] \boldsymbol{\varepsilon}_{e,0}^{n_i,m} \\
\boldsymbol{\varepsilon}_e^{n_i,u} &= [\boldsymbol{I} + \alpha \boldsymbol{C}_e^{0-1} (\boldsymbol{C}_{e,0}^0 - \boldsymbol{C}_e^0)] \boldsymbol{\varepsilon}_{e,0}^{n_i,u} \\
\boldsymbol{\varepsilon}_e^{n_i,s} &= [\boldsymbol{I} + \alpha \boldsymbol{C}_e^{1-1} (\boldsymbol{C}_{e,0}^1 - \boldsymbol{C}_e^1)] \boldsymbol{\varepsilon}_{e,0}^{n_i,s}
\end{aligned} \tag{26}$$

where $\boldsymbol{C}^{0}_{e,0}$ and $\boldsymbol{C}^{1}_{e,0}$ are unrotated planar and transverse stiffness matrices in the e^{th} design cell, and $\boldsymbol{\varepsilon}^{n_i m}_{e,0}$, $\boldsymbol{\varepsilon}^{n_i u}_{e,0}$, and $\boldsymbol{\varepsilon}^{n_i s}_{e,0}$ are element strain vectors of the e^{th} element before material rotations take place. They can be evaluated through finite element analysis at each iteration. Here, α is defined as the energy factor. When $\alpha = 0$, the energy based method degenerates into the strain based method, and it becomes the stress method when $\alpha = 1$. In this work, α is chosen as 0.75 for best performance. Detailed information about the energy based method and a comparison of the above three methods is given by Luo and Gea (1998).

Instead of employing Eq. 25 to obtain the mean-eigenvalue sensitivity information for the orientation variables $\theta_e (e = 1,2, \cdots, nd)$, the optimal orientations are directly computed through solving their optimality conditions. The optimality conditions for orientation variables to maximize the mean-eigenvalue Λ are

$$\frac{\partial \Lambda}{\partial \theta_e} = 0 \tag{27}$$

The roots of Eq. 27 can be found by making use of both Eq. 25 and Eq. 26. Of all the roots, the one making Λ largest is the optimal orientation.

V. OPTIMIZATION TECHNIQUE

The optimization problem is solved interactively via a two-level procedure of redesign. The eigenvalues and eigenvectors of the specified modes, as well as the corresponding equivalent strain vectors, are determined by finite element analysis in each loop of redesign. Improved orientations of the fibers are subsequently determined by means of the energy based method in the first level of the redesign. In the second level of redesign distributions of fibers are improved via sensitivity computation and a mathematical programming approach, called the generalized convex approach (Chickermane and Gea 1996). The sensitivity computation is based on the design determined just before the first level of redesign. The iterative procedure is continued until a stationary design is obtained. The initial design for the optimization process is normally taken to have the available amount of fiber uniformly distributed and oriented.

VI. NUMERICAL EXAMPLES

Two numerical examples are presented. The first example is to find the best stiffener configurations of a rectangular plate, in order to maximize its first, second, and third eigenfrequencies. The second example is to explore the opti-

mal stiffener design for a cantilevered square plate, with the objective of attaining the highest second and third eigenfrequencies.

A. Example 1

A rectangular plate of dimension $0.4m \times 0.3m$ is fixed at its four corner points, as shown in Fig. 2. Young's modulus of the plate is $E_m = 0.2Gpa$, Poisson's ratio is $\nu_m = 0.3$, and density is $\rho_m = 1000kg/m^3$. The plate has a constant thickness of $0.1cm$. The plate is discretized with a 40×30 finite element mesh and has 1200 CQUAD4 shell elements. After performing modal analysis, its first three eigenfrequencies are found to be $1.4981Hz$, $3.0860Hz$, and $3.6576Hz$. The corresponding mode shapes are shown in Fig. 3. The first plate mode is a bending mode, which deforms the plate in the direction of its longer side. The second mode is a twisting mode, and the third is a bending mode of higher order. In the latter two modes, the primary deformation occurs along the longer side of rectangular plate.

In order to achieve the maximum increase in the first three eigenfrequencies, stiffeners need to be placed in an optimal manner. The material properties of fiber, which is used to simulate stiffeners, are assumed to be Young's modulus $E_f = 20Gpa$, Poisson's ratio $\nu_f = 0.3$, and density $\rho_f = 1000kg/m^3$. The volume of available fiber is 1/4 of the total design space. The initial design is constructed by allocating the available fiber material evenly into each design element, and setting fiber orientation uniformly to be vertical. Figure 4 presents the final stiffener pattern, after 50 iterations (finite element analysis). In those elements where most fiber is present, the fiber density reaches its upper bound. Otherwise the fiber density drops to its lower bound. As can be seen, two symmetric arch stiffeners are formed between supporting points to best sustain the bending

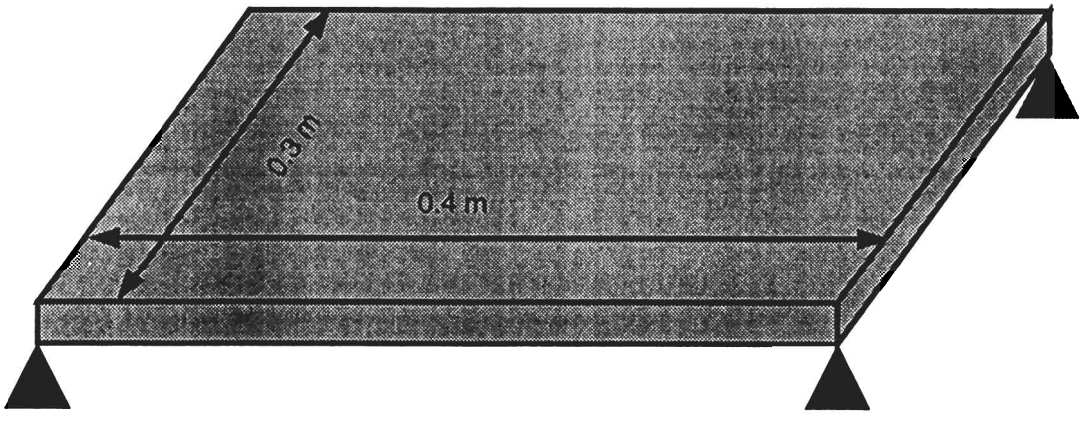

Fig. 2. Rectangular plate fixed at four corner points.

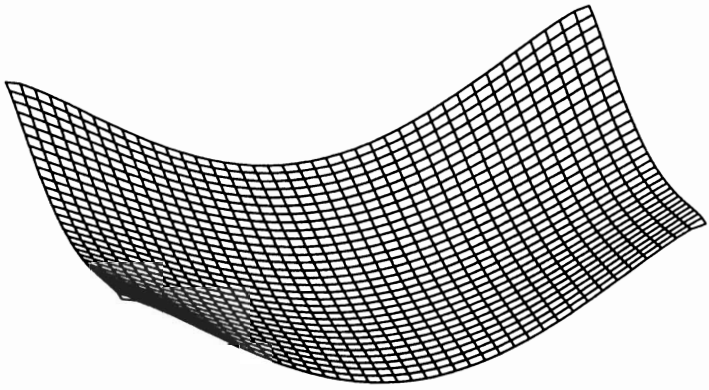

(a) First mode shape of rectangular plate

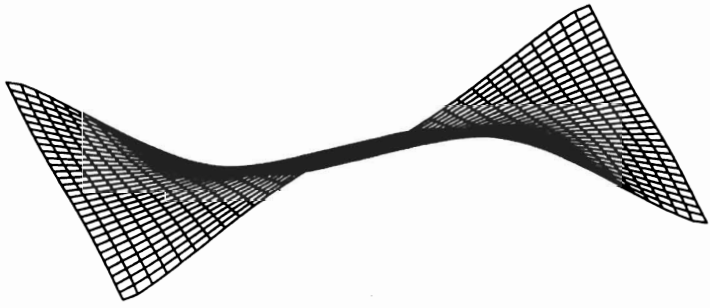

(b) Second mode shape of rectangular plate

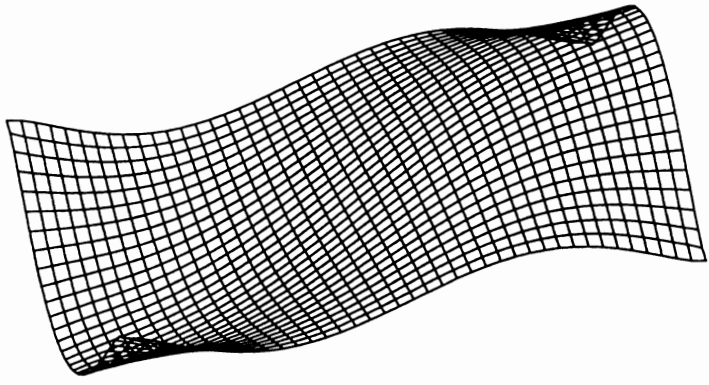

(c) Third mode shape of rectangular plate

Fig. 3. The first three mode shapes of rectangular plate without stiffeners.

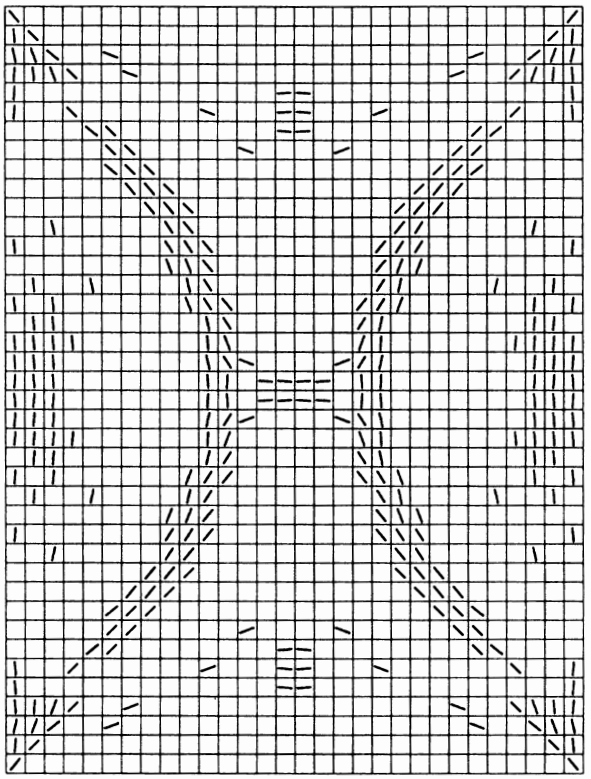

Fig. 4. Stiffener layout of rectangular plate for maximizing the first, second, and third eigenfrequencies.

modes. The occurrence of a bridge stiffener between two arches and some other stiffeners is to prevent the torsion mode from taking place at low frequency. The convergence histories of each eigenfrequency are depicted in Fig. 5. As shown in Table 1, the first eigenfrequency is increased from $2.7555Hz$ to $7.7798Hz$, the second eigenfrequency is increased from $4.7857Hz$ to $15.6943Hz$, and the third eigenfrequency achieves a final value of $16.4900Hz$, compared to its initial value of $7.2850Hz$.

B. Example 2

In the second example, consider the optimal stiffener design for a cantilever square plate to maximize the second and third eigenfrequencies simultaneously. The plate is of dimension $0.4m \times 0.4m$, as shown in Fig. 6. The plate thickness is $0.1cm$. The material properties of this square plate are Young's modulus $E_m = 0.2Gpa$, Poisson's ratio $\nu_m = 0.3$, and density $\rho_m = 1000kg/m^3$. In order to perform modal analysis of the square plate using the finite element method, the plate is discretized into a 40×40 mesh and has 1600 CQUAD4 shell elements.

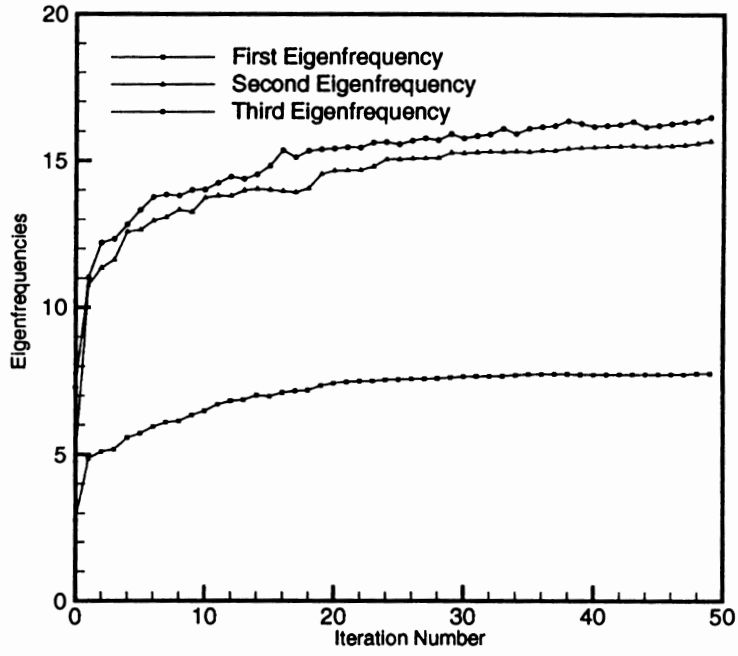

Fig. 5. Iteration history for maximizing the first, second, and third eigenfrequencies of rectangular plate.

The first mode is a simple bending mode with frequency $4.6724Hz$. The second mode is a twisting mode in which the plate vibrates anti-symmetrically with respect to the line connecting the centers of the fixed and free ends. The eigenfrequency of this mode is $11.4441Hz$. The third mode is a bending mode of higher order. The eigenfrequency of this mode is $28.6705Hz$.

The stiffener is simulated by fiber having Young's modulus $E_f = 20Gpa$, Poisson's ratio $\nu_f = 0.3$, and density $\rho_f = 1000kg/m^3$. The volume of available fiber is 1/4 of the whole structure. The initial design is formed by assigning fiber material uniformly to each design element and making the fiber orientation vertical. The first three eigenfrequencies of this initial design are $4.9503Hz$,

TABLE 1

Comparison of the first three eigenfrequencies of example 1.

Eigenfrequency	Non-stiffener design	Uniform design	Final design
ω_1	1.4981	2.7555	7.7796
ω_2	3.0860	4.7857	15.6943
ω_3	3.6576	7.2850	16.4900

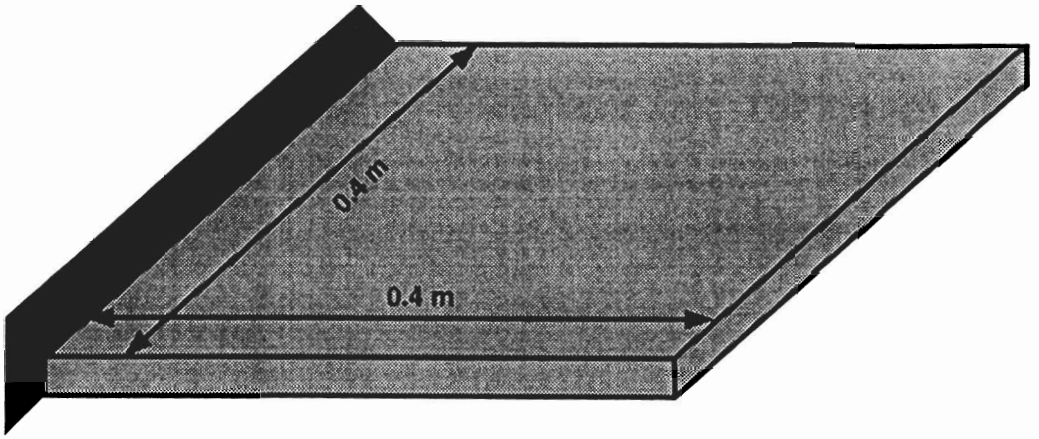

Fig. 6. Cantilever square plate.

14.0780Hz, and 31.0389Hz. Figure 7 shows the final stiffener configuration, after 50 iterations. The fibers are mainly accumulated in the path connecting the center of the free end to the central points of other two plate edges. The fiber orientations are 45 degrees with respect to the horizontal line. This build-up is necessary to increase the eigenfrequency of the torsion mode. Another finding in Fig. 8 is that some fibers occur in the vicinity of fixed end, with horizontal orientations. This mainly contributes to an increase in bending mode eigenfrequencies. The first three eigenfrequencies corresponding to the final design are 15.4646Hz, 51.20229Hz, and 123.6374Hz. Table 2, presents the first three eigenfrequencies for comparison. The second and third eigenvalues have been elevated significantly, compared to the initial design. The first eigenfrequency also experienced a moderate increase. The convergence history of the second and third eigenfrequencies is shown in Fig. 9.

It should be noted that repeated eigenfrequencies might occur in some problems. In that case, the repeated values are incorporated into the mean eigenvalue as the objective function. Notice that for individual repeated eigenfrequencies, the sensitivity does not exist. However, the sum of repeated eigenfrequencies is differentiable. Therefore, the above formulation still holds for the repeated eigenvalue problem.

VII. CONCLUSIONS

An automated topology optimization based approach has been developed to find the optimal stiffener pattern of shell structures, with the goal of maximizing a band of structural eigenvalues. The fiber-reinforced composite model is em-

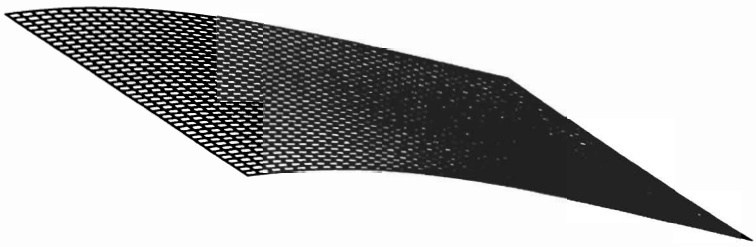

(a) First mode shape of square plate

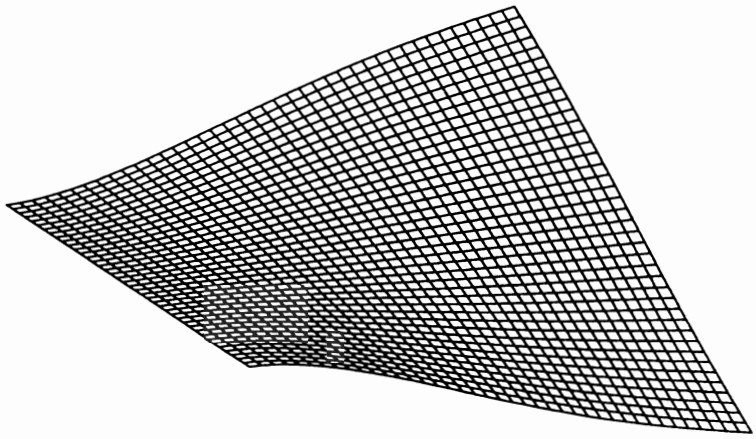

(b) Second mode shape of square plate

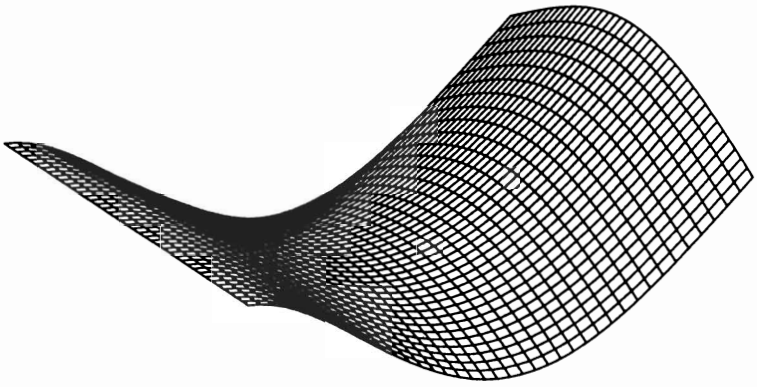

(c) Third mode shape of square plate

Fig. 7. The first three mode shapes of cantilever square plate without stiffeners.

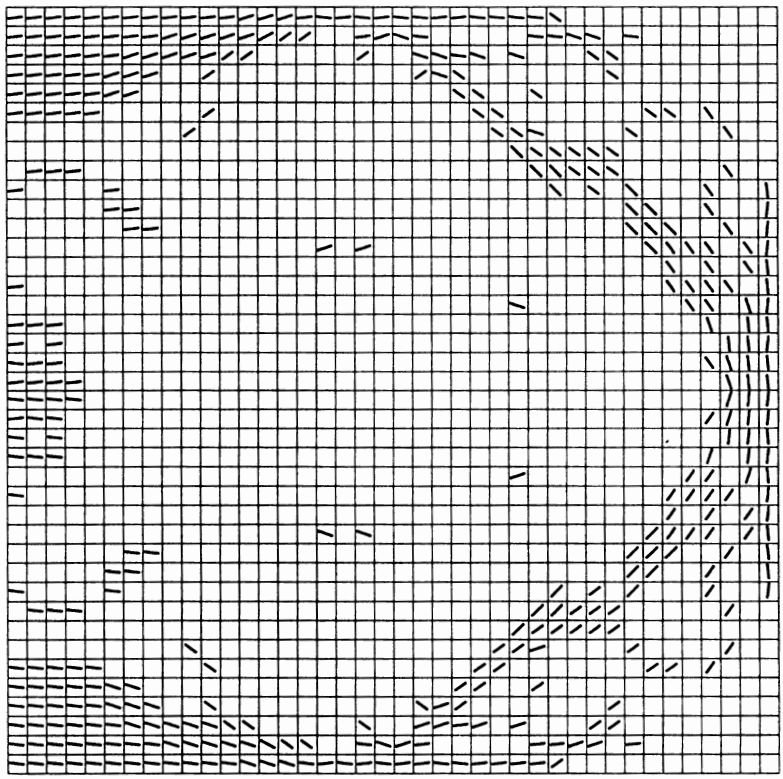

Fig. 8. Stiffener layout of square plate for maximizing the second and third eigenfrequencies.

ployed to simulate the stiffened structure, and the Composite Cylinder Assembly model is used to evaluate the elastic constants. The method is based on an iterative, two-level optimization procedure. In the first level, stiffener orientation is calculated using an optimality criterion. In the second level, stiffener density is computed by a mathematical programming approach, using analytical sensitivity information. Two numerical examples demonstrate the proposed method.

TABLE 2

Comparison of the first three eigenfrequencies of example 2.

Eigenfrequency	Non-stiffener design	Uniform design	Final design
ω_1	4.6724	4.9503	15.4646
ω_2	11.4441	14.0780	51.2029
ω_3	28.6705	31.0389	123.6374

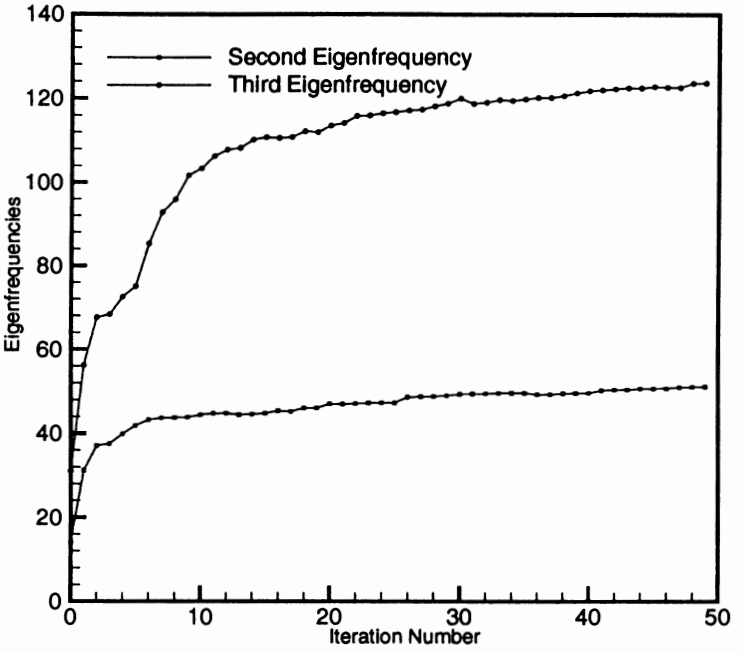

Fig. 9. Iteration history for maximizing the second and third eigenfrequencies of square plate.

Results show that significant improvement in the specified eigenvalues can be achieved by allocating and orienting the stiffener properly.

REFERENCES

1. A. R. Diaz and N. Kikuchi, Solutions to shape and topology eigenvalue optimization problems using a homogenization method, *International Journal for Numerical Methods in Engineering*, **35**:1487–1502 (1992).
2. Z. D. Ma, N. Kikuchi and I. Hagiwara, Structural topology and shape optimization for a frequency response problem, *Computational Mechanics*, **13**:157–174 (1993).
3. M. P. Bendsøe and N. Kikuchi, 1988, Generating optimal topologies in structural design using a homogenization method, *Computer Methods in Applied Mechanics and Engineering*, **71**: 197–224 (1988).
4. P. Pedersen, On Optimal orientation of orthotropic materials, *Structural Optimization*, **1**:101–106 (1989).
5. P. Pedersen, Bounds of elastic energy in solids of orthotropic materials, *Structural Optimization*, **2**:55–63 (1990).
6. J. Thomsen, Optimization of composite discs, *Structural Optimization*, **3**:89–98 (1991).
7. Z. Hashin and B. W. Rosen, The Elastic moduli of fiber-reinforced materials, *Journal of Applied Mechanics*, **31**:223–232 (1964).
8. R. M. Christensen and K. H. Lo, Solutions for effective shear properties in three phase sphere and cylinder models, *J. Mech. Phys. Solids*, **27**:315–330 (1979).

9. E. J. Haug, V. Komkov and K. K. Choi, *Designing Sensitivity Analysis of Structural Systems*, Academic Press, 1986.
10. A. R. Diaz and M. P. Bendsøe, Shape optimization of structures for multiple loading conditions using a homogenization method, *Structural Optimization*, **4**:17–22 (1992).
11. H. C. Cheng, N. Kikuchi, and Z. D. Ma, An improved approach for determining the optimal orientation of orthotropic material, *Structural Optimization*, **8**:101–112 (1994).
12. J. H. Luo and H. C. Gea, Optimal orientation of orthotropic materials using an energy based method, *Structural Optimization*, **15**:230–236 (1998).
13. H. Chickermane and H. C. Gea, A new local function approximation method for structural optimization problems, *International Journal for Numerical Methods in Engineering*, **39**:829–846 (1996).

Received May 1998
Revised September 1998